The proteome of distal nerves: implication in delayed repair and poor functional recovery

Song Guo[1], Raymond M. Moore[2], M. Cristine Charlesworth[3], Kenneth L. Johnson[3], Robert J. Spinner[1], Anthony J. Windebank[4], Huan Wang[1, *]

From the Contents

Graphical Abstract *Key proteins and pathways associated with poor nerve regeneration in chronic denervation*
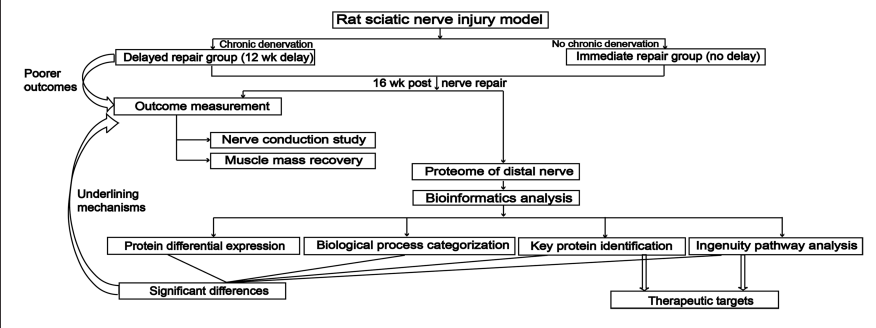
Abstract

Chronic denervation is one of the key factors that affect nerve regeneration. Chronic axotomy deteriorates the distal nerve stump, causes protein changes, and renders the microenvironment less permissive for regeneration. Some of these factors/proteins have been individually studied. To better delineate the comprehensive protein expression profiles and identify proteins that contribute to or are associated with this detrimental effect, we carried out a proteomic analysis of the distal nerve using an established delayed rat sciatic nerve repair model. Four rats that received immediate repair after sciatic nerve transection served as control, whereas four rats in the experimental group (chronic denervation) had their sciatic nerve repaired after a 12-week delay. All the rats were sacrificed after 16 weeks to harvest the distal nerves for extracting proteins. Twenty-five micrograms of protein from each sample were fractionated in SDS-PAGE gels. NanoLC-MS/MS analysis was applied to the gels. Protein expression levels of nerves on the surgery side were compared to those on the contralateral side. Any protein with a *P* value of less than 0.05 and a fold change of 4 or higher was deemed differentially expressed. All the differentially expressed proteins in both groups were further stratified according to the biological processes. A PubMed search was also conducted to identify the differentially expressed proteins that have been reported to be either beneficial or detrimental to nerve regeneration. Ingenuity Pathway Analysis (IPA) software was used for pathway analysis. The results showed that 709 differentially expressed proteins were identified in the delayed repair group, with a bigger proportion of immune and inflammatory process-related proteins and a smaller proportion of proteins related to axon regeneration and lipid metabolism in comparison to the control group where 478 differentially expressed proteins were identified. The experimental group also had more beneficial proteins that were downregulated and more detrimental proteins that were upregulated. IPA revealed that protective pathways such as LXR/RXR, acute phase response, RAC, ERK/MAPK, CNTF, IL-6, and FGF signaling were inhibited in the delayed repair group, whereas three detrimental pathways, including the complement system, PTEN, and apoptosis signaling, were activated. An available database of the adult rodent sciatic nerve was used to assign protein changes to specific cell types. The poor regeneration seen in the delayed repair group could be associated with the down-regulation of beneficial proteins and up-regulation of detrimental proteins. The proteins and pathways identified in this study may offer clues for future studies to identify therapeutic targets.

Key Words: chronic axotomy; chronic denervation; delayed repair; distal nerve; functional recovery; nerve regeneration; peripheral nerve; prolonged denervation; proteome; sciatic nerve; sciatic nerve transection

Introduction

Many factors, including the patient's age, type of trauma, and level of injury, can affect regeneration and functional recovery following nerve repair. Another critical prognostic factor is the timing of nerve repair. Prompt intervention is more effective than delayed intervention in restoring function (Mackinnon, 1989). However, immediate repair is oftentimes not possible due to concomitant injuries, infections, and late presentation. Functional recovery is compromised in patients whose nerve repair is delayed (Fu and Gordon, 1995; Samii et al., 2003; Han et al., 2015). The relatively poor clinical outcomes of delayed repair are generally attributed to atrophy of the denervated muscles (Anzil and Wernig, 1989). Additionally, chronic axotomy and chronic denervation significantly reduce the success of axonal regeneration (Fu and Gordon, 1995; Sulaiman et al., 2002). The decline in regenerative capacity corresponds to the decline in brain-derived neurotrophic factor

[1]Department of Neurologic Surgery, Mayo Clinic, Rochester, MN, USA; [2]Biomedical Statistics and Informatics, Mayo Clinic, Rochester, MN, USA; [3]Proteomics Core, Mayo Clinic, Rochester, MN, USA; [4]Department of Neurology, Mayo Clinic, Rochester, MN, USA
*Correspondence to: Huan Wang, MD, PhD, wang.huan@mayo.edu.
https://orcid.org/0000-0002-5540-0648 (Huan Wang)

(Sendtner et al., 1992), glial cell line-derived neurotrophic factor (Kotzbauer et al., 1996), and neurotrophin 4/5 (English et al., 2005) in the distal nerve that has been subject to chronic denervation. After losing axonal contact, denervated Schwann cells switch from a myelinating phenotype to a growth-supportive phenotype in which many regeneration-related genes are upregulated. However, the permissive factors decline with chronic denervation. This progressive decline and shift of denervated Schwann cells to a dormant state impact the migration of Schwann cells and their capacity to support axonal outgrowth (Fu and Gordon, 1997; Sulaiman et al., 2013). Prolonged denervation is also associated with the gradual loss of extracellular matrix structures.

Identifying the proteome profiles of the chronically denervated nerves can reveal more therapeutic targets to overcome the negative effects of chronic axotomy and chronic denervation. Studies focused on proteomic analyses of rat sciatic nerve transection injury, the most common model in nerve regeneration research, have been reported. Aiki et al. (2018) found that protein expression changes were site (proximal or distal) and stage (post-nerve transection time) specific after rat sciatic nerve transection: the number of identified proteins successively increased in both the proximal and distal stumps at 5, 10, and 35 days after injury. In the study by Bryan et al. (2012), the expression of 15 proteins known to be involved in various aspects of the regenerative process including growth factors, extracellular matrix (ECM) proteins, and adhesion and motility proteins was profiled in a 1 cm rat sciatic nerve conduit repair model over a 28-day regeneration period. They also showed that protein expression changes were site (proximal, within the conduit, or distal) and stage (earlier or later) specific (Bryan et al., 2012). Vergara et al. (2018) performed proteomic analysis on cross-sections of rat sciatic nerve at 20 days after nerve transection and immediate repair and identified 201 differentially expressed proteins that belonged to four significantly enriched canonical pathways: EIF2 signaling, LXR/RXR activation, acute phase response signaling and actin cytoskeleton signaling. To the best of our knowledge, there has not been a report about differential proteome profiling of promptly repaired and delayed repaired nerves. In this study, we used the established delayed rat sciatic nerve repair model to compare the proteomes between chronically and nonchronically axotomized nerves via label-free proteomics analysis to identify proteins that are potentially detrimental or beneficial to nerve regeneration.

Materials and Methods

Animal group assignment, surgery, and postoperative testing
The study was approved by the Institutional Animal Care and Use Committee (IACUC) of Mayo Clinic (protocol number A8814-14). All animal care and study procedures were carried out in accordance with the guidelines of NIH (National Institute of Health), USDA (United States Department of Agriculture), and AAALAC (Association for Assessment and Accreditation of Laboratory Animal Care International). Eight adult male Lewis rats (Harlan Laboratories, Indianapolis, IN, USA) with a body weight of around 200 g (ranging from 192 to 225 g) were included in this study. They were kept on a 12-hour light/12-hour dark cycle in an animal room, where they had free access to food and water. The rats were randomly allocated to the immediate repair group (n = 4) and the delayed repair group (n = 4) using the random number generator. The delayed repair group was used to establish the chronic denervation model, while the immediate repair group was regarded as the control group.

Rats underwent all surgical and postoperative evaluation/tissue harvest procedures under anesthesia with an intraperitoneal injection of 80 mg/kg ketamine (Ketaset III; Fort Dodge Animal Health, Fort Dodge, IA, USA) and 5 mg/kg xylazine (AnaSed; Lloyd Laboratories, Shenandoah, IA, USA). The surgical procedures were done under sterile conditions. Rats in the immediate repair group underwent one survival surgery. The left sciatic nerve was exposed at the posterior mid-thigh level and transected 12 mm distal to the lower border of the obturator tendon. The proximal and distal nerve stumps were instantly re-approximated after sciatic nerve transection and directly coapted with 10-0 monofilament nylon sutures (Ethilon, Ethicon Inc., New Brunswick, NJ, USA). Rats in the delayed repair group underwent two survival surgeries as previously described (Wu et al., 2013). In the first surgery, the proximal nerve stump was turned around and embedded into the neighboring muscles after sciatic nerve transection. The distal nerve stump was tagged 10 mm from the lower edge of the obturator tendon to prevent retraction. The incision was closed layer by layer. The second surgery was done

12 weeks later when the sciatic nerve was exposed again to mobilize the proximal and distal nerve ends which were trimmed and sutured together directly without tension. Postoperative pain management included a single dosage of subcutaneous injection of 0.05 mg/kg long-lasting buprenorphine (Buprenorphine Hydrochloride Injection III, Hospira, Lake Forest, IL, USA), supplemented by 30 mL Tylenol (Children's Mapap, Livonia, MI, USA) in every 473 mL of drinking water that started 48 hours preoperatively and lasted 7 days postoperatively.

Sixteen weeks after the nerve repair, a nerve conduction study was carried out in all the rats to record compound muscle action potential (CMAP) from muscles innervated by the two sciatic nerve branches, the tibial nerve and peroneal nerve using Nicolet Viking IV (Viasys Healthcare, Madison, WI, USA) (Wu et al., 2013). Each recording was repeated twice to ensure reproducibility. The average of the amplitude and latency of CMAP recorded from tibial nerve innervated muscle (Tamp and Tlat, respectively) and the average of the amplitude and latency of CMAP recorded from peroneal nerve innervated muscle (Pamp and Plat, respectively) from the two repeats were logged. After the nerve conduction study before the animal was euthanized, the tibialis anterior muscle and triceps surae muscle from both hind limbs were harvested and weighed using a digital balance (Mettler Toledo, Columbus, OH, USA). Wet muscle weight recovery was calculated by dividing the muscle weight on the operated side by the muscle weight on the contralateral side and expressed as a percentage. The mean and standard deviation of both CAMP data and muscle wet weight recovery data were calculated for each group.

Nerve sample processing for proteomics
After muscle harvest, the rats were euthanized and transcardially perfused with chilled 0.9% saline to expel any hematogenous components from the nerve samples. Sciatic nerves from both the surgical side and the contralateral normal side were harvested from the repair site to its muscle entry site and snap-frozen in liquid nitrogen. All nerve samples were stored at –80°C for later use.

Preparation of SDS-PAGE Gels
Each nerve segment, while still frozen, was transferred to a 0.5 mL 1.4 mm ceramic bead tube (Bertin Technologies, Green Bay, WI, USA) containing 100 μL lysis buffer (0.5% SDS, 0.5 mM MgCl$_2$, 20 mM Tris (pH 8.2), benzonase, Halt protease inhibitor). Tissue was homogenized twice at 5000 rpm for 30 seconds each using a Minilys bead beater (Bertin Technologies, Green Bay, WI, USA). The bead tubes were spun briefly, and the lysate was transferred to a 1.5 mL tube. The bead tubes were washed once with 50 μL of lysis buffer, which was also transferred to the new tubes. Samples were heated at 80°C for 10 minutes to denature the proteins. The protein concentration was determined by bicinchoninic acid (BCA) protein assay (Thermo Fisher Scientific Inc., Waltham, MA, USA) using bovine serum albumin (BSA) as a standard. Samples were frozen at –80°C until they needed to be thawed for electrophoresis.

SDS-PAGE and protein staining
Nerve lysate samples containing equal amounts of protein (5 μg) were dried on a vacuum centrifuge (Savant SpeedVac model SPD111V, Thermo Fisher Scientific, Waltham, MA, USA) and resolubilized in 30 μL of Laemmli buffer/5% beta-mercaptoethanol. After being heated for 10 minutes at 85°C, each sample was loaded on a 10.5–14% Criterion gel (Bio-Rad Laboratories, Hercules, CA, USA). Two pairs of lysates from nerves of the surgical side and contralateral side from each group (immediate repair and delayed repair), for a total of 8 samples, were run per gel. Electrophoresis was performed for 12 minutes at 140 V and 50 minutes at 200 V. Gels were fixed in 50% methanol/10% acetic acid for 30 minutes, and then stained for 1 hour with BioSafe Coomassie stain. Six horizontal, uniform sections across all the lanes on each gel were cut for individual tryptic digestion, peptide extraction, and mass spectrometry.

Protein identification by nano-scale liquid chromatography-tandem mass spectrometry
Gel sections from each lane were divided into approximately 1 mm cubes and digested with trypsin largely as previously described (Hogan et al., 2014). Gel sections were destained, reduced with tris(2-carboxyethyl)phosphine (TCEP), and alkylated with iodoacetamide. Then, 150 ng of sequencing-grade trypsin (Promega, Madison, WI, USA) was added to each sample, and the

samples were incubated overnight at 37°C. After digestion, peptides were first acidified with 10 μL of 4% trifluoroacetic acid (TFA) and then incubated for 30 minutes, after which the supernatant was transferred to new PCR tubes. A second extraction was performed with 60 μL acetonitrile (ACN) for 30 minutes, and the product was added to the first extract. The extracts were vacuum concentrated to dryness and stored at −80°C for LC-MS/MS analysis. LC-MS/MS measurements were performed by gel section using a data-dependent method on a Q-Exactive (Thermo Fisher Scientific Inc., Waltham, MA, USA) interfaced to a Dionex Ultimate® 3000 RSLCnano liquid chromatography as previously described (Ayers-Ringler et al., 2016). Dried tryptic peptides from each gel section were reconstituted in 50 μL of an aqueous solution of 0.2% formic acid (FA), 0.1% TFA, and 0.002% Zwittergent 3–16. The autosampler was used to load sample aliquots (10 μL for gel sections A, B, and C; 5 μL for gel section D; 15 μL for gel sections E and F) that were preconcentrated on a 0.25 μL reversed-phase OptiPak trap (Optimize Technologies, Oregon City, OR, USA) custom-packed with 5 μm, 200 Å Magic C8 stationary phase (Bruker-Michrom, Auburn, CA, USA). Peptides were washed for 4 minutes at 10 μL/minute with aqueous 0.2% FA and 0.05% TFA, and the trap was then placed in line with the analytical column via a 10-port valve. Peptides were separated on a 40 cm long, 100 μm internal diameter self-packed PicoFrit® (NewObjective, Woburn, MA, USA) column packed with Poroshell 120S EC-C18, 2.7 μm stationary phase (Agilent, Santa Clara, CA, USA). A mobile phase gradient of 2–30% over 70 minutes (phase A), followed by a 30–50% gradient over 30 minutes (phase B), was used at a flow rate of 400 nL/min, where mobile phase A was 2% ACN in high-performance liquid chromatography grade water (Honeywell Burdick & Jackson, Muskegon, MI, USA) with 0.2% FA and mobile phase B was ACN/isopropanol/water (80/10/10 by volume) with overall 0.2% FA. Eluting peptides were electrosprayed from the column tip into the Q-Exactive mass spectrometer, where MS1 scans over the m/z range of 350–2000 were recorded at 70,000 resolving power (measured at m/z 200) using an AGC (automatic gain control) value of 3E6. Tandem mass spectra (MS2) were recorded for the 15 most abundant multiply charged precursors (fragment ions recorded with 17,500 resolving power, AGC=2E5, NCE (normalized collision energy) =26, fixed first m/z of 140, maximum ion fill time of 50 ms, isolation window of 3 m/z, isolation offset of 0.5 m/z, 60-second dynamic exclusion).

Bioinformatic analysis of label-free differential expression using LC-MS/MS data

We utilized a label-free peptide MS1 intensity-based method for finding differentially expressed proteins between the operated side and the contralateral side. All MS/MS were matched against a composite mouse protein sequence database containing the UniProt reference proteome (downloaded June 2015, https://www.uniprot.org/proteomes/) and sequences of common contaminants (e.g., trypsin, keratin, cotton, wool). Reversed protein sequences were appended to the database to estimate the false discovery rates (FDRs) of protein identification. First, we utilized our MyriMatch-IDPicker-SwiftQA in-house pipeline to assess the quality of the raw LC-MS/MS data (Ma et al., 2009; Tabb et al., 2007). For this purpose, MyriMatch was configured to derive semitryptic peptides from the protein database while matching the MS/MS present in a run. The MyriMatch software was configured to use 10 ppm m/z tolerance when matching both precursor and fragment ions. MyriMatch also considered the following variable modifications for the search: carbamidomethylation of cysteine (+57.023 Da), oxidation of methionine (+15.994 Da), and n-terminal pyroglutamic acid (-17.023 Da). IDPicker (Ma et al., 2009) filtered the resulting peptide-spectrum matches at a 2% FDR and assembled them into protein identifications. SwiftQA processed the raw spectra and identified peptides to extract quality metrics (such as mass error of identified peptides, total ion current of acquired MS and MS/MS scans, mass error drift with retention time, and quality of the acquired and identified MS/MS) associated with each LC-MS/MS run. Runs whose quality control metrics were within expected ranges (determined based on historical yeast lysate LC-MS/MS runs) were considered for peptide intensity quantification. All LC-MS/MS analyses present in this study met the quality assurance criteria. A previously published MaxQuant-based (version 1.5.1, https://www.maxquant.org) protocol was utilized to detect the peptides and proteins present in each sample and record their intensities (Cox and Mann, 2008; Cox et al., 2014). The software was configured to use 20 ppm m/z tolerance for precursors and fragments while performing peptide-spectrum matching. The software derived semitryptic peptides from the aforementioned protein sequence database while searching for the above-described variable modifications, augmented to include protein n-terminal acetylation (+42.01 Da). MaxQuant filtered the peptide and protein identifications at a 1% FDR, grouped protein identifications into groups, and reported protein group intensities.

Data analysis
Statistical analysis
No statistical methods were used to predetermine sample sizes; however, our sample sizes are similar to those reported in previous publications (Aiki et al., 2018; Vergara et al., 2018). An in-house script written in the programming language R (version 3.1.2) was utilized to perform differential expression analysis of the detected protein group intensities between the samples for any two experimental groups of interest. For this purpose, the protein group intensities of each sample were log2 transformed and normalized using the quantile method (Bolstad et al., 2003). For each protein group, the normalized intensities observed in the comparative groups of samples were modeled using a Gaussian-linked generalized linear model (Nelder and Wedderburn, 1972). A one-way analysis of variance was used to detect the differentially expressed proteins between a pair of experimental groups. Differential expression p-values were FDR corrected using the Benjamini-Hochberg-Yekutieli procedure (Benjamini and Hochberg, 1995). Protein groups with a corrected *P*-value of ≤ 0.05 and an absolute log2 fold change of ≥ 4 (where 0.0 signifies no change) were considered significantly differentially expressed. Independent-sample t-tests were performed using SPSS software (version 19.0, SPSS Inc., Chicago, IL, USA) to evaluate nerve conduction and wet muscle weight data. *P*-values of less than 0.05 were considered significant.

Biological process & pathway analysis
Ingenuity Pathway Analysis (IPA, build version 389077M, Licensed by Qiagen, a multi-national company headquartered in Hilden, Germany) was used to analyze the proteins identified as significantly different by the bioinformatic analysis described above. The ratios, *P*-values, and FDRs from these resulting proteins were uploaded to IPA with their corresponding UniProt identifiers. The Disease and Functions algorithm was used to determine the significantly enriched terms between the immediate repair group and the delayed repair group. Additionally, the pathway and network functions were used to identify the top pathways most likely to have been impacted.

Results

Nerve conduction study and wet muscle weight recovery
The nerve conduction study data were summarized in **Table 1**. The amplitudes of CMAPs recorded from both the tibial nerve and peroneal nerve innervated muscles were significantly lower in the delayed repair group compared with the immediate repair group (*P* < 0.05), reflecting poor reinnervation. Conversely, CMAP latencies (especially latency of CAMP recorded from tibial nerve innervated muscle) were significantly longer in the delayed repair group which is indicative of slower conduction.

Table 1 │ Nerve conduction study of the chronic denervation (delayed repair) and the non-chronic denervation (immediate repair) groups

Group	CMAP amplitudes		CMAP latencies	
	Tamp (mV)	Pamp (mV)	Tlat (ms)	Plat (ms)
Immediate repair	7.53±1.93	9.63±1.12	1.68±0.25	1.68±0.28
Delayed repair	1.31±0.50*	1.59±0.64*	2.21±0.09*	2.08±0.30

Data are expressed as mean ± SD of each group (*n* = 4). **P < 0.05, *vs.* immediate repair group (independent-sample *t*-tests). SD: Standard deviation; Tamp: amplitude of CMAP recorded from tibial nerve innervated muscle; Pamp: amplitude of CMAP recorded from peroneal nerve innervated muscle; Tlat: latency of CAMP recorded from tibial nerve innervated muscle; Plat: latency of CMAP recorded from peroneal nerve innervated muscle; CMAP: compound muscle action potential.

The wet muscle weight recovery of the triceps surae was 71% on average in the immediate repair group and 45% in the delayed repair group, whereas these of the tibialis anterior were 80% and 48% on average, respectively. Muscle mass recovery was significantly worse in the delayed repair rats (**Table 2**).

Table 2 | The wet muscle weight recovery of chronic denervation (delayed repair) and non-chronic denervation (immediate repair) groups

Group	TS recovery (%)	TA recovery (%)
Immediate repair	70.81±8.90	79.60±11.65
Delayed repair	45.43±8.20[*]	47.89±15.82[*]

[*]$P < 0.05$, *vs*. immediate repair group (independent-sample *t*-tests). Data were expressed as mean ± SD of each group (*n* = 4). SD: Standard deviation; TS: triceps surae muscle; TA: tibialis anterior muscle.

Protein expression profile in the distal sciatic nerve

Each distal nerve proteome contained 5754 detectable proteins on the surgical side and contralateral side from both groups (immediate repair and delayed repair). To identify proteins that were differentially expressed, the relative abundance measured by mass spectrometry was compared between nerve samples (*n* = 8) of the surgery side from both immediate and delayed repair groups and nerve samples (*n* = 8) of the contralateral side from both groups. All the expression levels of such identified proteins were compared among the above groups to screen out the proteins with significant change using a P-value less than 0.05. Such proteins with a statistically significant change were further analyzed from the biological perspective to make the analysis biologically meaningful. Therefore, a fold change threshold was determined by analyzing the characteristics of protein expression profile between the operated side and contralateral side in all 8 rats, since nerve transection and repair surgery could be regarded as a notable biological factor and should lead to significant protein profile changes compared to the contralateral intact nerve. The comparative analysis between the surgery side and the contralateral side showed an apparent natural break point at a 4-fold change (**Figure 1**). This natural break point was probably caused by the biological factor, namely, nerve transection and repair surgery. The threshold for differential expression was therefore arbitrarily defined as a 4-fold change and a *P*-value less than 0.05.
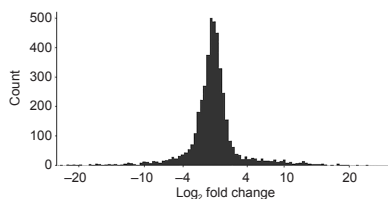

Figure 1 | Comparative analysis of identified protein spots between nerve samples from the surgical repair side and nerve samples from the contralateral side.
The proteins were congregated and plotted by fold changes when positive values indicate an up-regulated fold change in the repair side nerve compared to its contralateral side counterpart and negative values indicate a down-regulated fold change. This figure shows a natural break point at a 4-fold change. The threshold for differential expression was therefore set as 4 fold change and a *P*-value less than 0.05.

Further comparison of the protein profiles of the surgery side nerve samples to the contralateral side samples in the immediate repair group revealed that 270 proteins were significantly downregulated and 208 proteins were upregulated, while the comparison of protein profiles of nerve samples of the surgery side to those of the contralateral side in the delayed repair group revealed 392 significantly downregulated and 317 upregulated proteins. Comparative analysis of the protein profiles of the surgery side nerve samples in the immediate repair group and the surgery side samples in the delayed repair group revealed 104 proteins that were significantly downregulated and 77 proteins that were significantly upregulated (**Figure 2**).

Biological processes and key proteins

The differentially expressed proteins in either the immediate repair group or the delayed repair group were assigned to subcategories according to the biological function they are associated with. Six biological processes associated with nerve regeneration were identified: inflammatory response, cell proliferation, cell migration, cell apoptosis, axon regeneration, and lipid metabolism. Some of the proteins were involved in multiple processes and assigned to more than one process group. The percentages of differentially expressed proteins that were associated with such afore-mentioned biological processes in the immediate repair group were inflammatory
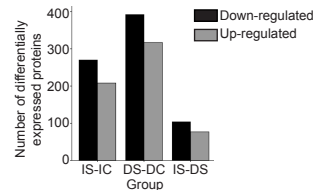

Figure 2 | Overview of the differentially expressed proteins between samples for any two sets of interest.
The bar graph on the left shows the number of identified proteins that were differentially expressed when comparing samples (*n* = 4) of the surgical side to samples (*n* = 4) of the contralateral side in the immediate repair group, as defined by a fold change of more than 4 and a *P*-value of less than 0.05. The bar graph in the middle shows the number of identified proteins that were differentially expressed when comparing samples (*n* = 4) of the surgical side to samples (*n* = 4) of the contralateral side in the delayed repair group. The bar graph on the right represents the number of identified proteins that were differentially expressed when comparing samples (*n* = 4) of the surgical side in the immediate repair group to samples (*n* = 4) of the surgical side in the delayed repair group. IS-IC, DS-DC, IS-DS mean IS *vs*. IC, DS *vs*. DC, IS *vs*. DS, respectively. DC: Delayed repair contralateral side; DS: delayed repair surgery side; IC: immediate repair contralateral side; IS: Immediate repair surgery side.

response 5.89%, cell proliferation 33.89%, cell migration 15.16%, cell apoptosis 22.95%, axon regeneration 6.32% and lipid metabolism 15.78%, respectively. While, similar percentages in the delayed repair group were 12.93%, 32.93%, 16.73%, 22.59%, 2.31% and 12.52%, respectively (**Figure 3**). When comparing the percentages of biological processes between the immediate repair and delayed repair groups, we found that the inflammatory response process was increased in the delayed repair group, while axon regeneration processes were decreased. In the delayed repair group, 69/95 differentially expressed proteins related to the inflammatory response process were upregulated and 26/95 were down-regulated, while 6/17 differentially expressed proteins related to axon regeneration were upregulated and 11/17 were down-regulated. In the immediate repair group, 12/28 differentially expressed proteins related to the inflammatory response process were upregulated and 16/28 were down-regulated, while 14/30 differentially expressed proteins related to axon regeneration were upregulated and 16/30 were down-regulated.
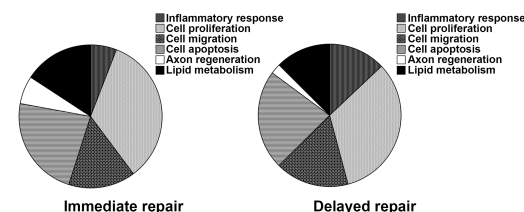

Figure 3 | Biological process analysis of differentially expressed proteins.
Pie charts showing functional groups as a fraction of differentially expressed (either up-regulated or down-regulated when comparing surgery side to contralateral side) proteins in the immediate nerve repair group and delayed nerve repair group. In the delayed repair group there were more proteins belonging to the biological process of immune/inflammatory response and fewer proteins pertaining to axon outgrowth and lipid metabolism processes.

Furthermore, we analyzed the differentially expressed proteins by searching the literature to identify the proteins that are related to the key processes in nerve injury and regeneration. Multiple key proteins were identified to be involved in the inflammatory response, cell proliferation, cell apoptosis, cell migration, axon regeneration, and lipid metabolism processes (**Table 3**). The differential expressions of these key proteins, either up-regulation or down-regulation, in the aforementioned processes were listed in **Additional Tables 1–6** and shown in the heatmap (**Figure 4**). By comparing fold change expression levels between surgery side samples in the immediate repair group to surgery side samples in the delayed repair group, we identified the top three differentially expressed proteins in each of the biological processes. The top three differentially expressed proteins in the inflammatory response process were S100A8, PLA2G4A, and S100A9, which were all up-regulated in the nerves that have been subjected to chronic denervation. The top three differentially expressed proteins in the

Table 3 │ Proteins related to the various biological processes that were identified to be differentially expressed

Biological process	Key proteins
Inflammatory response	S100A8 (Chernov et al., 2015), S100A9 (Chernov et al., 2015), PLA2G4A (López-Vales et al., 2008), CBL (Kohno et al., 2011; Seon et al., 2018), LIMK1 (Endo et al., 2003; Koch et al., 2014), MPZ (Lemke and Axel, 1985; Giese et al., 1992), PTGDS (Trimarco et al., 2014), CD63 (Chernousov et al., 2013), POSTN (Shimamura et al., 2012; Shih et al., 2014; Matsunaga et al., 2015), RAB27A (Chen et al., 2012), SFRP1 (Kele et al., 2012)
Cell proliferation	MAPK11 (Fragoso et al., 2003; Hossain et al., 2012), CASP6 (Monnier et al., 2011), S100A8 (Chernov et al., 2015), IGFBP5 (Simon et al., 2015), S100A9 (Chernov et al., 2015), MSLN (Roet et al., 2013), SPAST (Wood et al., 2006; Butler et al., 2010), SHH (Martinez et al., 2015), LIMK1 (Endo et al., 2003; Koch et al., 2014), GJB1 (Scherer et al., 1998), DHH (Bajestan et al., 2006), HSPB8 (Zhang et al., 2014), CBL (Kohno et al. 2011; Seon et al., 2018), MADD (Hao et al., 2010), MPZ (Lemke et al., 1985; Giese et al., 1992), IGF1R (Joshi et al., 2015; Jeon et al., 2017), PTGDS (Trimarco et al., 2014), ARHGAP24 (Nguyen et al., 2012), CD63 (Chernousov et al., 2013), APOD (Ganfornina et al., 2010), CASP3 (Saito et al., 2009), RAB27A (Chen et al., 2012), SFRP1 (Kele et al., 2012), EGR2 (Decker et al., 2006), POSTN (Shimamura et al., 2012; Shih et al., 2014; Matsunaga et al., 2015)
Cell apoptosis	MAPK11 (Fragoso et al., 2003; Hossain et al., 2012), APOD (Ganfornina et al., 2010), C6 (Ramaglia et al., 2009), CASP3 (Saito et al., 2009), RAB27A (Chen et al., 2012), SFRP1 (Kele et al., 2012), EGR2 (Decker et al., 2006), POSTN (Shimamura et al., 2012; Shih et al., 2014; Matsunaga et al., 2015), CASP6 (Monnier et al., 2011), S100A8 (Chernov et al., 2015), IGFBP5 (Simon et al., 2015), NFIB (Betancourt et al., 2014), S100A9 (Chernov et al., 2015), SMURF1 (Kannan et al., 2012), SHH (Martinez et al., 2015), CNTF (Sahenk et al., 1994; Newman et al., 1996), GJB1 (Scherer et al., 1998), PAK3 (Hing et al., 1999), HSPB8 (Zhang et al., 2014), CBL (Kohno et al., 2011; Seon et al., 2018), LGALS8 (Pardo et al., 2019), IGF1R (Joshi et al., 2015; Jeon et al., 2017), PTGDS (Trimarco et al., 2014), MPZ (Lemke et al., 1985; Giese et al., 1992), MADD (Hao et al., 2010), CAMKK1 (Ageta-Ishihara et al., 2009)
Cell migration	S100A8 (Chernov et al., 2015), S100A9 (Chernov et al., 2015), LIMK1 (Endo et al., 2003; Koch et al., 2014), MPZ (Lemke et al., 1985; Giese et al., 1992), PTGDS (Trimarco et al., 2014), ADGRG6 (Monk et al., 2011), EGR2 (Decker et al., 2006), ITGB2 (Feltri et al., 2002), TXNIP (Sbai et al., 2010), LYN (Hossain et al., 2010), RAB27A (Chen et al., 2012), SFRP1 (Kele et al., 2012), C6 (Ramaglia et al., 2009), EPHB2 (Parrinello et al., 2010), CD63 (Chernousov et al., 2013)
Axon regeneration	SMURF1 (Kannan et al., 2012), SPAST (Wood et al., 2006; Butler et al., 2010), SHH (Martinez et al., 2015), CNTF (Sahenk et al., 1994; Newman et al., 1996), LIMK1 (Endo et al., 2003; Koch et al., 2014), GJB1 (Scherer et al., 1998), PAK3 (Hing et al., 1999), HSPB8 (Zhang et al., 2014), ARPP19 (Irwin et al., 2002), IGF1R (Joshi et al., 2015; Jeon et al., 2017), MPZ (Lemke et al., 1985; Giese et al., 1992), CAMKK1 (Ageta-Ishihara et al., 2009), CASP6 (Monnier et al., 2011), CASP3 (Saito et al., 2009), SYNPO (Vlachos et al., 2009), EGR2 (Decker et al., 2006), NTN1 (Madison et al., 2000)
Lipid metabolism	S100A9 (Chernov et al., 2015), S100A8 (Chernov et al., 2015), APOD (Ganfornina et al., 2010), RAB27A (Chen et al., 2012), CASP3 (Saito et al., 2009), CNTF (Sahenk et al., 1994; Newman et al., 1996), LIMK1 (Endo et al., 2003; Koch et al., 2014), DHH (Bajestan et al., 2006), CBL (Kohno et al., 2011; Seon et al., 2018), LGALS8 (Pardo et al., 2019), IGF1R (Joshi et al., 2015; Jeon et al., 2017), PTGDS (Trimarco et al., 2014), TRPV1 (Ren et al., 2015)

Figure 4 │ Heatmaps of key regulatory proteins involved in the designated biological processes.
Differentially expressed proteins were identified by comparing samples of the surgery side in the immediate repair group to samples of the surgery side in the delayed repair group (IS-DS), comparing samples of the surgery side to samples of the contralateral side in the delayed repair group (DS-DC), and comparing samples of the surgery side to samples of the contralateral side in the immediate repair group (IS-IC). Positive fold changes of protein expression level represent up-regulation and are shown in red colors. Negative fold changes represent down-regulation and are shown in green colors. DC: Delayed repair contralateral side; DS: delayed repair surgery side; IC: immediate repair contralateral side; IS: immediate repair surgery side.

cell proliferation process were S100A8, MSLN, and S100A9, which were all up-regulated in the nerves that have been subjected to chronic denervation. The top three differentially expressed proteins in the cell apoptosis process were S100A8, S100A9, and MAPK11, with MAPK11 down-regulated and the other two up-regulated in the nerves that have been subjected to chronic denervation. The top three differentially expressed proteins in the cell migration process were S100A8, S100A9, and CD63, with S100A8 and S100A9 significantly up-regulated in the nerves that have been subjected to chronic denervation. The top three differentially expressed proteins in the axon regeneration process were CAMKK1, MPZ, and IGF1R, which were all significantly down-regulated in the nerves that have been subjected to chronic denervation. The top three
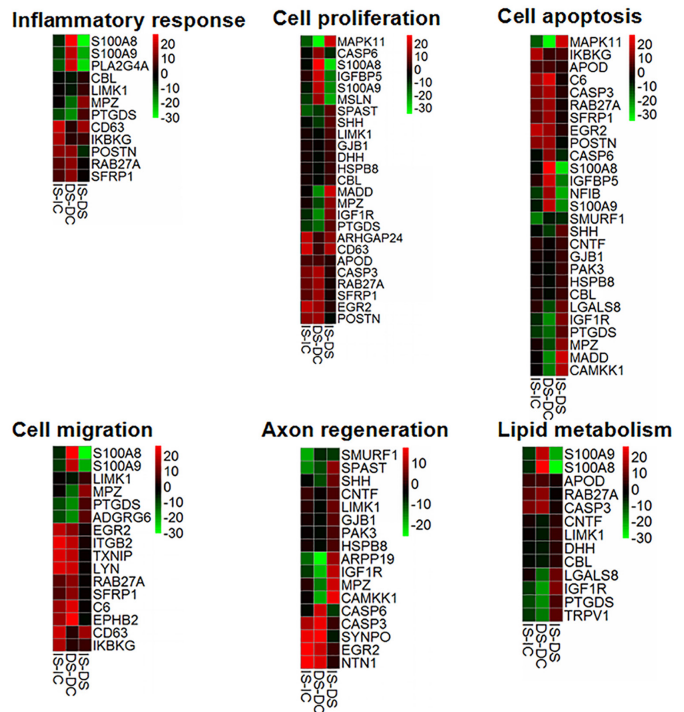
differentially expressed proteins in the lipid metabolism process were S100A8, S100A9, and IGF1R, with IGF1R down-regulated and the other two up-regulated in the nerves that have been subjected to chronic denervation. Among these key proteins, some were beneficial to nerve regeneration while others were detrimental. The differential expression of these beneficial or detrimental proteins might lead to the difference in nerve regeneration ability between the immediate repair and delayed repair groups. Therefore, the differential expression of proteins associated with nerve regeneration was further analyzed as shown in **Figure 5**. In the immediate repair group, ten beneficial proteins, namely, POSTN (Shimamura et al., 2012; Shih et al., 2014; Matsunaga et al., 2015), ARHGAP24 (Nguyen et al., 2012), SYNPO (Vlachos et al., 2009), NTN1 (Madison et al., 2000), EGR2 (Decker et al., 2006), LYN (Hossain et al., 2010), CD63 (Chernousov et al., 2013), EPHB2 (Parrinello et al., 2010), TXNIP (Sbai et al., 2010) and APOD (Ganfornina et al., 2010), and one detrimental protein C6 (Ramaglia et al., 2009) were upregulated; while eight beneficial proteins, namely, SPAST (Wood et al., 2006; Butler et al., 2010), SHH (Martinez et al., 2015), CAMKK1 (Ageta-Ishihara et al., 2009), MSLN (Roet et al., 2013), SMURF1 (Kannan et al., 2012), NFIB (Betancourt et al., 2014), PTGDS (Trimarco et al., 2014) and MAPK11 (Fragoso et al., 2003; Hossain et al., 2012), and two detrimental proteins PLA2G4A (López-Vales et al., 2008) and TRPV1 (Ren et al., 2015) were downregulated. In the delayed repair group, nine beneficial proteins, namely, RAB27A (Chen et al., 2012), NTN1 (Madison et al., 2000), SYNPO (Vlachos et al., 2009), LYN (Hossain et al., 2010), TXNIP (Sbai et al., 2010), EPHB2 (Parrinello et al., 2010), MSLN (Roet et al., 2013), APOD (Ganfornina et al., 2010) and POSTN (Shimamura et al., 2012; Shih et al., 2014; Matsunaga et al., 2015), and eight detrimental proteins, namely, S100A8 (Chernov et al., 2015), S100A9 (Chernov et al., 2015), PLA2G4A (López-Vales et al., 2008), CASP6 (Monnier et al., 2011), CASP3 (Saito et al., 2009), IGFBP5 (Simon et al., 2015), C6 (Ramaglia et al., 2009) and SFRP1 (Kele et al., 2012) were upregulated; while 15 beneficial proteins, namely, SHH (Martinez et al., 2015), LGALS8 (Pardo et al., 2019), PAK3 (Hing et al., 1999), CNTF (Sahenk et al., 1994; Newman and Verity, 1996),
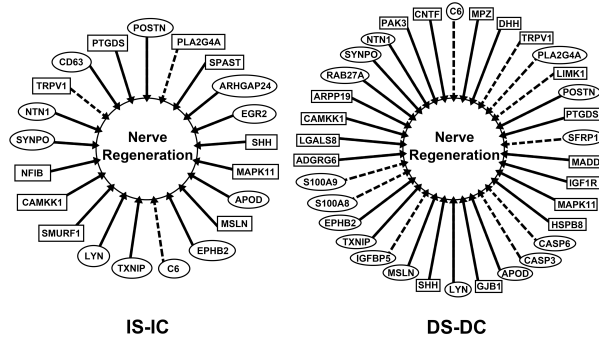
Figure 5 | The impact of the key proteins on nerve regeneration.
The diagram indicated the key proteins that were identified in the immediate repair group (IS-IC) and delayed repair group (DS-DC) and their roles on nerve regeneration. In the immediate repair group, ten beneficial proteins, CD63, POSTN, ARHGAP24, EGR2, APOD, EPHB2, TXNIP, LYN, SYNPO, and NTN1 were up-regulated and two detrimental proteins, PLA2G4A, and TRPV1, were downregulated. In the delayed repair group, fifteen beneficial proteins, MPZ, PTGDS, MADD, IGF1R, DHH, HSPB8, GJB1, SHH, MAPK11, ADGRG6, LGALS8, PAK3, CNTF, CAMKK1, and ARPP19 were downregulated, while, eight detrimental proteins, S100A8, S100A9, SFRP1, PLA2G4A, CASP6, CASP3, IGFBP5, and C6 were upregulated. Oval represents upregulation; Rectangle represents downregulation; Solid lines and dashed lines, respectively, represent the activating and inhibitory effects of the corresponding proteins on nerve regeneration. DC: Delayed repair contralateral side; DS: delayed repair surgery side; IC: immediate repair contralateral side; IS: immediate repair surgery side.

CAMKK1 (Ageta-Ishihara et al., 2009), MADD (Hao et al., 2010), IGF1R (Jeon et al., 2017; Joshi et al., 2015), ARPP19 (Irwin et al., 2002), MPZ (Giese et al., 1992; Lemke and Axel, 1985), PTGDS (Trimarco et al., 2014), DHH (Bajestan et al., 2006), HSPB8 (Zhang et al., 2014), GJB1 (Scherer et al., 1998), MAPK11 (Fragoso et al., 2003; Hossain et al., 2012) and ADGRG6 (Monk et al., 2011), and two detrimental proteins TRPV1 (Ren et al., 2015) and LIMK1 (Endo et al., 2003; Koch et al., 2014) were downregulated.

Cell types for key proteins
The "sciatic nerve ATlas" (https://snat.ethz.ch/index.html), was used to further refine protein classification. The resource is an openly accessible online resource which was established through the transcriptional profiling of mouse sciatic nerve at the single-cell level (Gerber et al., 2021). This dataset contained the analysis of cells at early postnatal development (P1) and cells at the adult stage (P60) using single-cell RNA sequencing of sciatic nerve cells. Using the search function of this database we looked at the gene cluster and differential expression of the previously identified genes of interest across epineurial cells, perineurial cells, endoneurial cells, endothelial cells, immune cells, Remak and myelinating Schwann cells, pericytes, and vascular smooth muscle cells in age P60 sciatic nerve plots. The appearance of a violin plot in the expression level plot indicated that the P-value of the gene of interest in the specific cell cluster was less than 0.05 and this gene was considered to be differentially enriched in this cell cluster. After inputting genes of all the key proteins, we found that 19 key proteins could be assigned to at least one cell type of the sciatic nerve (**Table 4**). Organizing these key proteins by cell types revealed that each cell type had multiple enriched key proteins. The greatest number of enriched key proteins were seen in pericytes and endothelial cells (**Table 5**). Further organizing these enriched key proteins into the experimental (delayed repair) and control (immediate repair) groups showed that two of the 19 key proteins, SFRP1 and IGFBP5, were upregulated detrimental proteins and only seen differentially expressed in the delayed repair group (**Table 6**).

Canonical pathways analysis
All the differentially expressed proteins were uploaded to the IPA dataset for canonical pathways analysis. Sixty-five canonical pathways were significantly regulated in the immediate repair group (**Additional Figure 1**). By IPA analysis, 5 pathways were predicted to be activated, and 17 pathways were predicted to be inhibited. The roles of the 22 pathways in nerve regeneration were further confirmed by searching Pubmed. We found that the signaling pathways that were related to nerve regeneration were calcium signaling, LXR/RXR activation, protein kinase A signaling, and IL-6 signaling. Concerning the activation status of the above pathways in the immediate repair group, LXR/RXR activation was predicted to be

Table 4 | Key proteins that were assigned to sciatic nerve cells

Key protein	Cells
MSLN	PnC
MPZ	SC
EGR2	SC
DHH	SC
MADD	Per/EC
SYNPO	Per/EC
LGALS8	Per/EC
SFRP1	EpC, PnC
HSPB8	EpC, EC1
LYN	IC, Per/EC
NTN1	EpC, PnC
POSTN	EpC, PnC, Per/EC
IGF1R	EC1, Per/EC, Per/VSMC
IGFBP5	EpC, EnC, PnC, EC2, Per/EC, Per/VSMC
TXNIP	SC, EpC, EnC, IC, EC1, EC2, Per/EC, Per/VSMC
NFIB	SC, EpC, EnC, PnC, EC1, EC2, Per/EC, Per/VSMC
CD63	SC, EpC, EnC, PnC, IC, EC1, EC2, Per/EC, Per/VSMC
APOD	SC, EpC, EnC, PnC, IC, EC1, EC2, Per/EC, Per/VSMC
ARPP19	SC, EpC, EnC, PnC, IC, EC1, EC2 Per/EC, Per/VSMC

EC: Endothelial cells including EC1 and EC2; EnC: endoneurial cells; EpC: epineurial cells; IC: immune cells; Per/VSMC: pericytes and vascular smooth muscle cells; Per/EC: pericytes and endothelial cells; PnC: perineurial cells; SC: Schwann cells.

Table 5 | The cell types in the sciatic nerve and the key proteins assigned to each cell type

Cells	Key protein
SC	MPZ, EGR2, DHH, TXNIP, NFIB, CD63, APOD, ARPP19
EpC	SFRP1, HSPB8, NTN1, POSTN, IGFBP5, TXNIP, NFIB, CD63, APOD, ARPP19
EnC	IGFBP5, TXNIP, NFIB, CD63, APOD, ARPP19
PnC	MSLN, SFRP1, NTN1, POSTN, IGFBP5, NFIB, CD63, APOD, ARPP19
IC	LYN, TXNIP, CD63, APOD, ARPP19
EC1	HSPB8, IGF1R, TXNIP, NFIB, CD63, APOD, ARPP19
EC2	IGFBP5, TXNIP, NFIB, CD63, APOD, ARPP19
Per/EC	MADD, SYNPO, LGALS8, LYN, POSTN, IGF1R, IGFBP5, TXNIP, NFIB, CD63, APOD, ARPP19
Per/VSMC	IGF1R, IGFBP5, TXNIP, NFIB, CD63, APOD, ARPP19

EC: Endothelial cells including EC1 and EC2; EnC: endoneurial cells; EpC: epineurial cells; IC: immune cells; Per/VSMC: pericytes and vascular smooth muscle cells; Per/EC: pericytes and endothelial cells; PnC: perineurial cells; SC: Schwann cells.

Table 6 | Enriched proteins in various sciatic nerve cell types that are differentially expressed in the delayed repair and immediate repair groups

Cell type	Delayed repair	Immediate repair
SC	MPZ, DHH, **TXNIP**, **APOD**, ARPP19	EGR2, NFIB, **TXNIP**, **CD63**, APOD
EpC	*SFRP1*, HSPB8, **NTN1**, **POSTN**, *IGFBP5*, **TXNIP**, ARPP19	NTN1, **POSTN**, **TXNIP**, NFIB, **CD63**, **APOD**
EnC	*IGFBP5*, **TXNIP**, **APOD**, ARPP19,	**TXNIP**, NFIB, **CD63**, **APOD**
PnC	**MSLN**, *SFRP1*, **NTN1**, **POSTN**, *IGFBP5*, **TXNIP**, ARPP19	MSLN, **NTN1**, **POSTN**, **TXNIP**, NFIB, **CD63**, **APOD**
IC	**LYN**, **TXNIP**, **APOD**, ARPP19	**LYN**, **TXNIP**, **CD63**, **APOD**
EC1	HSPB8, IGF1R, **TXNIP**, **APOD**, ARPP19	**TXNIP**, NFIB, **CD63**, **APOD**
EC2	*IGFBP5*, **TXNIP**, ARPP19	**TXNIP**, NFIB, **CD63**, **APOD**
Per/EC	MADD, **SYNPO**, LGALS8, **LYN**, **POSTN**, IGF1R, *IGFBP5*, **TXNIP**, **APOD**, ARPP19	**SYNPO**, **LYN**, **POSTN**, **TXNIP**, NFIB, **CD63**, **APOD**
Per/VSMC	IGF1R, *IGFBP5*, **TXNIP**, **APOD**, ARPP19	**TXNIP**, NFIB, **CD63**, **APOD**

EC: Endothelial cells including EC1 and EC2; EnC: endoneurial cells; EpC: epineurial cells; IC: Immune cells; Per/VSMC: pericytes and vascular smooth muscle cells; Per/EC: pericytes and endothelial cells; PnC: perineurial cells; SC: Schwann cells. Italic font: Deteriorating proteins; regular font: beneficial proteins; bold font: upregulation; non-bold font: downregulation. Underlined proteins are an example of potentially important proteins congruously regulated across several cell types.

activated whereas the other three pathways were inhibited. Fifty-two canonical pathways were significantly regulated in the delayed repair group (**Additional Figure 2**). Using IPA analysis, 8 signaling pathways were predicted to be activated, and 21 signaling pathways were predicted to be inhibited. The signaling pathways that were related to nerve regeneration were LXR/RXR activation, acute phase response signaling, the complement system, PTEN signaling, Rac signaling, ERK/MAPK signaling, apoptosis signaling, CNTF signaling, IL-6 signaling, and FGF signaling. Concerning the activation status of the above pathways in the delayed repair group, the complement system pathway, PTEN signaling pathway, and apoptosis signaling pathway were predicted to be activated whereas the rest seven pathways were inhibited.

Discussion

In this study, we examined the proteomes of repaired nerves that have or have not been subject to chronic denervation. Poorer regeneration and functional recovery were seen in the chronic denervation group, reflected by nerve conduction study and wet muscle weight recovery study that showed prolonged CMAP latency, reduced CMAP amplitude, and decreased muscle mass restoration. This difference in outcomes was underlined by differences in the protein expression profiles. The observations of different levels of protein expression reflect the state of the proteomic environment at the time of the observation. These establish associations between a poor or detrimental, delayed repair and a successful or beneficial immediate repair condition. These cannot be interpreted as having a cause-and-effect relationship. Upregulation of certain proteins, e.g. myelin proteins may be markers or the result of successful regeneration. In addition, the heterogeneity of the cellular environment and proportion of various cells within the injured nerve increases the difficulty of assigning specific causal roles to individual proteins.

To approach this problem, we categorized the differentially expressed proteins according to the biological processes relevant to nerve injury and repair. This revealed a significantly bigger fraction of inflammatory process-related proteins and a significantly smaller fraction of proteins related to axonal regeneration and lipid metabolism processes in the delayed repair nerve proteome. Furthermore, over 70% of the inflammatory process proteins were up-regulated and over 60% of the axonal regeneration proteins were down-regulated in this group. This indicated a prolonged and more activated immune/inflammatory response in the chronic denervation model, whereas the axon regeneration process was decreased. These findings could be among the underlying mechanisms that contributed to the poorer outcomes in this group. One day after nerve injury inflammatory cytokines are secreted to advance the recruitment of blood-borne macrophages. The recruited macrophages induce the production and secretion of anti-inflammatory cytokines to gradually bring Wallerian degeneration to end (Rotshenker, 2011). This initial immune/inflammatory response is essential in clearing the way and creating a permissive environment for the extension of re-growing axons. The inflammatory process should not be dominant later on because it can be detrimental to nerve regeneration. Persistent hyperinflammatory state in aging sciatic nerves has been shown to diminish nerve regenerative capacity following injury by altering Schwann cell behavior that leads to a defective Schwann cell response (Büttner et al., 2018). Axon outgrowth is a crucial process for nerve regeneration. Its undermining can be caused by diminished expression of axon regeneration-related genes. This attests to the detrimental effect of chronic denervation.

We also identified the key proteins beneficial or detrimental to nerve regeneration which were differentially expressed in either the immediate repair group or the delayed repair group. The proteins thought to be beneficial to regeneration were POSTN, ARHGAP24, SYNPO, NTN1, EGR2, LYN, CD63, EPHB2, TXNIP, APOD, RAB27A, MSLN, SPAST, SHH, CAMKK1, SMURF1, NFIB, PTGDS, MAPK11, LGALS8, PAK3, CNTF, MADD, IGF1R, ARPP19, MPZ, DHH, HSPB8, GJB1, and ADGRG6. Studies have shown these proteins to play a positive role in neurite outgrowth (Nguyen et al., 2012; Roet et al., 2013; Shih et al., 2014; Matsunaga et al., 2015), neuroprotection (Shimamura et al., 2012; Jeon et al., 2017; Pardo et al., 2019), synaptic plasticity (Irwin et al., 2002; Vlachos et al., 2009), axonal guidance (Hing et al., 1999; Madison et al., 2000), axon outgrowth (Sahenk et al., 1994; Wood et al., 2006; Butler et al., 2010; Kannan et al., 2012; Betancourt et al., 2014; Joshi et al., 2015), onset and/or maintaining of myelination (Lemke and Axel, 1985; Giese et al., 1992;

Scherer et al., 1998; Fragoso et al., 2003; Decker et al., 2006; Hossain et al., 2010; Monk et al., 2011; Chen et al., 2012; Trimarco et al., 2014), Schwann cell differentiation (Hossain et al., 2012), Schwann cell migration along axons (Parrinello et al., 2010; Sbai et al., 2010; Chernousov et al., 2013), myelin clearance and macrophage recruitment (Ganfornina et al., 2010), outgrowth and branching of adult sensory neurons (Martinez et al., 2015), axonogenesis and dendritogenesis of immature cortical neurons (Ageta-Ishihara et al., 2009), and mitigating degeneration (Bajestan et al., 2006). The proteins thought to be detrimental to regeneration were PLA2G4A, TRPV1, C6, S100A8, S100A9, CASP6, CASP3, IGFBP5, SFRP1, and LIMK1. Studies have shown these proteins lead to a prolonged inflammatory response (López-Vales et al., 2008; Chernov, et al., 2015), impaired neurite and axon extension (Endo et al., 2003; Ren et al., 2015; Simon et al., 2015), activated complement system (Ramaglia et al., 2009), activated cell apoptosis (Saito et al., 2009; Monnier et al., 2011) and repressed neuritogenesis (Kele et al., 2012).

Although the dataset of Sciatic Nerve Atlas was derived from profiling mouse nerve, we used it in our attempt to assign the differentially expressed key proteins to cellular constituents of the sciatic nerve, because this has been the best available and most relevant dataset and because rat and mouse are both rodent species. This allows a first attempt at refining the cellular origins of the protein changes we observed.

Furthermore, the canonical pathway analysis also predicted differences in the key signaling pathways between the two groups. One signaling pathway, LXR/RXR activation, was activated and 3 pathways including calcium signaling, protein kinase A (PKA) signaling, and IL-6 signaling were inhibited in the immediate repair group. In the delayed repair group, seven pathways including CNTF signaling, IL-6 signaling, FGF signaling, LXR/RXR activation, acute phase response signaling, Rac signaling, and ERK/MAPK signaling were inhibited while three pathways including apoptosis signaling, PTEN signaling, and complement signaling were activated. Calcium signaling can affect events including cytoskeletal dynamics and local protein translation, transport and trafficking in the growth cone to promote nerve regeneration (Sonigra et al., 1999; Bradke et al., 2012; Vergara et al., 2018). PKA pathway plays an important role in axon outgrowth. Pharmacological elevation of cAMP, as a mediator, accelerated neurite outgrowth in cultured motoneurons by activating the cAMP-PKA axis (Gordon et al., 2010). The inhibition of these two pathways in the immediate repair group 16 weeks post-repair indicated a phase that passed early regeneration. The only activated key pathway in the immediate repair group was the LXR/RXR pathway. This pathway was involved in the regulation of lipid metabolism and transport. A prior study indicated the importance of lipid synthesis and transport for nerve regeneration (Yi et al., 2015). However, the LXR/RXR pathway, as the most enriched canonical pathway in the delayed repair group, was inhibited. The inhibition of this pathway in the delayed repair group was in accordance with the decreased lipid metabolism process seen in our results. Acute phase response signaling was the second most enriched canonical signaling pathway in the delayed repair group, which was also inhibited. A previous study showed that acute phase response signaling was initiated immediately after peripheral nerve injury to promote nerve regeneration (Yi et al., 2015). The complement system, the fourth most enriched canonical signaling pathway, was activated in the delayed repair group. A study showed that the inhibition of this pathway by C6 deletion accelerated axonal regeneration and functional recovery after sciatic nerve injury (Ramaglia et al., 2009). Prolonged activation of the complement system might be detrimental to nerve regeneration. Shin et al. reported that Rac-MKK7 pathway worked as an important pathway for the response of Schwann cells to peripheral nerve injury and promoting nerve regeneration (Shin et al., 2013). Newbern et al. demonstrated that activated ERK/MAPK signaling in Schwann cells could stimulate Schwann cell dedifferentiation *in vivo* to promote nerve regeneration. Inhibition of these two pathways in delayed repair could be detrimental. Moreover, the apoptosis signaling pathway was activated in the delayed repair group, which was consistent with the increase in proteins associated with the biological process of apoptosis. Inhibition of PTEN signaling could accelerate sciatic nerve regeneration by enhancing axon outgrowth (Christie et al., 2010). In the delayed repair group, this pathway was activated. Prior studies showed that CNTF, as a neurotrophic factor, could enhance peripheral and central nerve regeneration (Sahenk et al., 1994; Newman and Verity, 1996). Leibinger et al. (2013) demonstrated the contribution of IL-6 to CNS axon regeneration. IL-6/STAT3 signaling

in primary Schwann cells induced expression of the gene encoding glial fibrillary acidic protein which is required for proper regeneration of the injured peripheral nerve (Lee et al., 2009a, b). Hausott et al. indicated that FGF could promote peripheral and central nerve regeneration. The inhibition of CNTF, IL-6 and FGF signaling pathways in the delayed repair group could potentially contribute to poorer nerve regeneration.

There are several limitations in this proteomics study. First, only one time point 16 weeks after repair surgery was examined. The temporal changes in the protein profiles were not explored. The proteome only reflects the state the nerve was in when it was harvested. One could argue that the proteome of the nerve in the immediate repair group is expected to contain more beneficial proteins or fewer detrimental proteins since nerve regeneration is more complete and the nerve is in a better myelinated state. Vice versa for the proteome of the nerve in the delayed repair group. However, these trends do not predict causal relationships. Up to now, proteomic studies have mainly focused on nerve injury without repair (Aiki et al., 2018; Wei et al., 2020), or observed over 20 days or 28 days after immediate repair (Bryan et al., 2012; Vergara et al., 2018). Both key proteins and pathways that were identified in these studies differed from our proteomics findings. Our study is unique in that the nerve in our model has been subjected to chronic denervation before repair, which is a common yet challenging clinical scenario for nerve regeneration and functional restoration. A second limitation is the relatively small sample size. Third, to facilitate the analysis of such a large data set, we categorized all the differentially expressed proteins by biological processes. However, many key proteins functioned in more than one biological processes. The interactions of such proteins were not explored in this study, thus leading to a simplified analysis. Similarly, all the indicated pathways were analyzed separately, without considering signaling interactions. Four, identification of key proteins that are beneficial or detrimental to nerve regeneration was achieved by literature search using relevant key words. Given the fact that one protein can have multiple terminology by the genes that encode them, it was inevitable that some key proteins were missed during the search.

The process of refinement of gene categories that we used did result in the identification of a relatively small number of proteins that were differentially regulated in the poor or successful regeneration condition. Numbers were further restricted by using available databases to assign these proteins to specific cell types that are present in peripheral nerves. Future studies to address mechanistic relationships between proteins and success of regeneration may use secretome studies of individual cell types *in vitro*, that have been genetically modified to up or down-regulate specific proteins or factors.

Conclusions
This proteomics study demonstrated distinctively different protein profiles in the nerves that are repaired immediately and that are repaired after chronic denervation. As delayed nerve repair is commonly seen in the clinical practice with less ideal functional outcomes, future studies employing secretome proteomics that account for cellular composition in protein profiling can reveal potential therapeutic targets to improve the functional recovery.

Additional files:
Additional Table 1: *Differentially expressed key proteins relevant to the inflammatory response process in the chronic denervation (delayed repair) and the non-chronic denervation (immediate repair) groups.*
Additional Table 2: *Differentially expressed key proteins relevant to the cell proliferation process in the chronic denervation (delayed repair) and the non-chronic denervation (immediate repair) groups.*
Additional Table 3: *Differentially expressed key proteins relevant to the cell apoptosis process in the chronic denervation (delayed repair) and the non-chronic denervation (immediate repair) groups.*
Additional Table 4: *Differentially expressed key proteins relevant to the cell migration process of the chronic denervation (delayed repair) and the non-chronic denervation (immediate repair) groups.*
Additional Table 5: *Differentially expressed key proteins relevant to the axon regeneration process of the chronic denervation (delayed repair) and the non-chronic denervation (immediate repair) groups.*
Additional Table 6: *Differentially expressed key proteins relevant to the lipid metabolism process of the chronic denervation (delayed repair) and the non-chronic denervation (immediate repair) groups.*
Additional Figure 1: *Significantly regulated pathways in the immediate repair group.*
Additional Figure 2: *Significantly regulated pathways in the delayed repair group.*

References

Ageta-Ishihara N, Takemoto-Kimura S, Nonaka M, Adachi-Morishima A, Suzuki K, Kamijo S, Fujii H, Mano T, Blaeser F, Chatila TA., Mizuno H, Hirano T, Tagawa Y, Okuno H, Bito H (2009) Control of cortical axon elongation by a GABA-driven Ca2/calmodulin-dependent protein kinase cascade. J Neurosci 29:13720-13729.
Aiki H, Wada T, Iba k, Oki G, Sohma H, Yamashita T, Kokai Y (2018) Proteomics analysis of site- and stage-specific protein expression after peripheral nerve injury. J Orthop Sci 23:1070-1078.
Anzil AP, Wernig A (1989) Muscle fibre loss and reinnervation after long-term denervation. J Neurocytol 18:833-845.
Ayers-Ringler JR, Oliveros A, Qiu YY, Lindberg DM, Hinton DJ, Moore RM, Dasari S, Choi DS (2016) Label-free proteomic analysis of protein changes in the striatum during chronic ethanol use and early withdrawal. Front Behav Neurosci 10:46.
Bajestan SN, Umehara F, Shirahama Y, Itoh K, Sharghi-Namini S, Jessen KR, Mirsky R, Osame M (2006) Desert hedgehog-patched 2 expression in peripheral nerves during Wallerian degeneration and regeneration. J Neurobiol 66:243-255.
Benjamini Y, Hochberg Y (1995) Controlling the false discovery rate: A practical and powerful approach to multiple testing. J R Statist Soc B 57:289-300,
Betancourt J, Katzman S, Chen B (2014) Nuclear factor one B regulates neural stem cell differentiation and axonal projection of corticofugal neurons. J Comp Neurol 522:6-35.
Bolstad BM, Irizarry RA, Astrand M, Speed TP (2003) A comparison of normalization methods for high density oligonucleotide array data based on variance and bias. Bioinformatics 19:185-193.
Bradke F, Fawcett JW, Spira ME (2012) Assembly of a new growth cone after axotomy: the precursor to axon regeneration. Nat Rev Neurosci 13:183-193.
Bryan DJ, Litchfield CR, Manchio JV, Logvinenko T, Holway AH, Austin J, Summerhayes IC, Rieger-Christ KM (2012) Spatiotemporal expression profiling of proteins in rat sciatic nerve regeneration using reverse phase protein arrays. Proteome Sci 10:9.
Butler R, Wood JD, Landers JA, Cunliffe VT (2010) Genetic and chemical modulation of spastin-dependent axon outgrowth in zebrafish embryos indicates a role for impaired microtubule dynamics in hereditary spastic paraplegia. Dis Model Mech 3(11-12):743-751.
Büttner R, Schulz A, Reuter M, Akula AK, Mindos T, Carlstedt A, Riecken LB, Baader SL, Bauer R, Morrison H (2018) Inflammaging impairs peripheral nerve maintenance and regeneration. Aging Cell 17:e12833.
Chen G, Zhang ZJ, Wei ZY, Cheng Q, Li X, Li W, Duan SM, Gu XS (2012) Lysosomal exocytosis in schwann cells contributes to axon remyelination. Glia 60:295-305.
Chernousov MA, Richard CS, David JC, David JC (2013) Tetraspanins are involved in Schwann cell-axon interaction. J Neurosci Res 91:1419-1428.
Chernov AV, Jennifer D, Khang H, Mila A, Geetha S, Thomas V, Svetlana B, Alex YS, Veronica IS (2015) The calcium-binding proteins S100A8 and S100A9 initiate the early inflammatory program in injured peripheral nerves. J Biol Chem 290:11771-11784.
Christie KJ, Webber CA, Martinez JA, Singh B, Zochodne DW (2010) PTEN inhibition to facilitate intrinsic regenerative outgrowth of adult peripheral axons. J Neurosci 30:9306-9315.
Cox J, Hein MY, Luber CA, Paron I, Nagaraj N, Mann M (2014) Accurate proteome-wide label-free quantification by delayed normalization and maximal peptide ratio extraction, termed MaxLFQ. Mol Cell Proteomics 13:2513-2526.
Cox J, Mann M (2008) MaxQuant enables high peptide identification rates, individualized p.p.b.-range mass accuracies and proteome-wide protein quantification. Nat Biotechnol 26:1367-1372.
Decker L, Desmarquet-Trin-Dinh C, Taillebourg E, Ghislain J, Vallat JM, Charnay P (2006) Peripheral myelin maintenance is a dynamic process requiring constant Krox20 expression. J Neurosci 26:9771-9779.
Endo M, Ohashi K, Sasaki Y, Goshima Y, Niwa R, Uemura T, Mizuno K (2003) Control of growth cone motility and morphology by LIM kinase and Slingshot via phosphorylation and dephosphorylation of cofilin. J Neurosci 23:2527-2537.
English AW, Meador W, Carrasco DI (2005) Neurotrophin-4/5 is required for the early growth of regenerating axons in peripheral nerves. Eur J Neurosci 21:2624-2634.
Feltri ML, Porta GD, Previtali SC, Nodari A, Migliavacca B, Cassetti A, Littlewood-Evans A, Reichardt LF, Messing A, Quattrini A, Mueller U, Wrabetz L (2002) Conditional disruption of beta 1 integrin in Schwann cells impedes interactions with axons. J Cell Biol 156:199-209.
Fragoso G, Robertson J, Athlan E, Tam E, Almazan G, Mushynski WE (2003) Inhibition of p38 mitogen-activated protein kinase interferes with cell shape changes and gene expression associated with Schwann cell myelination. Exp Neurol 183:34-46.

Fu SY, Gordon T (1995) Contributing factors to poor functional recovery after delayed nerve repair: prolonged axotomy. J Neurosci 15:3876-3885.

Fu SY, Gordon T (1997) The cellular and molecular basis of peripheral nerve regeneration. Mol Neurobiol 14:67-116.

Ganfornina MD, Carmo SD Martínez E, Tolivia J, Navarro A, Rassart E, Sanchez D (2010) ApoD, a glia-derived apolipoprotein, is required for peripheral nerve functional integrity and a timely response to injury. Glia 58:1320-1334.

Gerber D, Pereira JA, Gerber J, Tan G, Dimitrieva S, Yánguez E, Suter U (2021) Transcriptional profiling of mouse peripheral nerves to the single-cell level to build a sciatic nerve ATlas (SNAT). Elife 10:e58591.

Giese KP, Martini R, Lemke G, Soriano P, Schachner M (1992) Mouse P0 gene disruption leads to hypomyelination, abnormal expression of recognition molecules, and degeneration of myelin and axons. Cell 71:565-576.

Gordon T, Amirjani N, Edwards DC, Chan KM (2010) Brief post-surgical electrical stimulation accelerates axon regeneration and muscle reinnervation without affecting the functional measures in carpal tunnel syndrome patients. Exp Neurol 223:192-202.

Han N, Xu CG, Wang TB, Kou YH, Yin XF, Zhang PX, Xue F (2015) Electrical stimulation does not enhance nerve regeneration if delayed after sciatic nerve injury: the role of fibrosis. Neural Regen Res 10:90-94.

Hao JC, Adler CE, Mebane L, Gertler FB, Bargmann CI, Tessier-Lavigne M (2010) The tripartite motif protein MADD-2 functions with the receptor UNC-40 (DCC) in Netrin-mediated axon attraction and branching. Dev Cell 18:950-960.

Hausott B, Rietzler A, Vallant N, Auer M, Haller I, Perkhofer S, Klimaschewski L (2011) Inhibition of fibroblast growth factor receptor 1 endocytosis promotes axonal branching of adult sensory neurons. Neuroscience 188:13-22.

Hing H, Xiao J, Harden N, Lim L, Zipursky SL (1999) Pak functions downstream of Dock to regulate photoreceptor axon guidance in Drosophila. Cell 97: 853-863.

Hogan MC, Johnson KL, Zenka RM, Charlesworth MC, Madden BJ, Mahoney DW, Oberg AL, Huang BW, Leontovich AA, Nesbitt LL, Bakeberg JL, McCormick DJ, Bergen HR, Ward CJ (2014) Subfractionation, characterization, and in-depth proteomic analysis of glomerular membrane vesicles in human urine. Kidney Int 85:1225-1237.

Hossain S, Cruz-Morcillo MA, Sanchez PR, Almazan G (2012) Mitogen activated protein kinase p38 regulates krox20 to direct schwann cell differentiation and peripheral myelination. Glia 60:1130-1144.

Hossain S, Fragoso G, Mushynski WE, Almazan G (2010) Regulation of peripheral myelination by Src-like kinases. Exp Neurol 26: 47-57.

Irwin N, Chao,S. Goritchenko L, Horiuchi A, Greengard P, Nairn AC, Benowitz LI (2002) Nerve growth factor controls GAP-43 mRNA stability via the phosphoprotein ARPP-19. Proc Natl Acad Sci U S A 99:12427-12431.

Jeon HJ, Park JH, Shin JH, Chang MS (2017) Insulin-like growth factor binding protein-6 released from human mesenchymal stem cells confers neuronal protection through IGF-1R-mediated signaling. Int J Mol Med 40:1860-1868.

Joshi Y, Sória MG, Quadrato G, Inak G, Zhou L, Hervera A, Rathore KI, Elnaggar M, Cucchiarini M, Marine JC, Puttagunta R, Giovanni SD (2015) The MDM4/MDM2-p53-IGF1 axis controls axonal regeneration, sprouting and functional recovery after CNS injury. Brain 138:1843-1862.

Kannan M, Lee SJ, Schwedhelm-Domeyer N, Nakazawa T, Stegmüller J (2012) The E3 ligase Cdh1-anaphase promoting complex operates upstream of the E3 ligase Smurf1 in the control of axon growth. Development 139:3600-3612.

Kele J, Andersson ER, Villaescusa JC, Cajanek CLP, Bonilla S, Toledo EM, Bryja V, Rubin JS, Shimono A, Arenas E (2012) SFRP1 and SFRP2 dose-dependently regulate midbrain dopamine neuron development in vivo and in embryonic stem cells. Stem Cells 30:865-875.

Koch JC, Tönges L, Barski E, Michel U, Bähr M, Lingor P (2014) ROCK2 is a major regulator of axonal degeneration, neuronal death and axonal regeneration in the CNS. Cell Death Dis 5:e1225.

Kohno S, Ueji T, Abe T, Nakao R, Hirasaka K, Oarada M, Harada-Sukeno A, Ohno A, Higashibata A, Mukai R, Terao J, Okumura Y, Nikawa T (2011) Rantes secreted from macrophages disturbs skeletal muscle regeneration after cardiotoxin injection in Cbl-b-deficient mice. Muscle Nerve 43:223-229.

Kotzbauer PT, Lampet PA, Heuckerotht RO, Golden JP, Creedon DJ, Johnson Jr EM, Milbrandt J (1996) Neurturin, a relative of glial-cell-line-derived neurotrophic factor. Nature 384:467-470.

Lee HK, Seo IA, Suh DH, Hong JI, Yoo YH, Park HT (2009a) Interleukin-6 is required for the early induction of glial fibrillary acidic protein in Schwann cells during Wallerian degeneration. J Neurochem 108:776-786.

Lee HK, Wang L, Shin YK, Lee YK, Yoo YH, Park HT (2009b) Interleukin-6 induces proinflammatory signaling in Schwann cells: a high-throughput analysis. Biochem Biophys Res Commun 382:410-414.

Leibinger M, Müller A, Gobrecht P, Diekmann H, Andreadaki A, Fischer D (2013) Interleukin-6 contributes to CNS axon regeneration upon inflammatory stimulation. Cell Death Dis 4:e609.

Lemke G, Axel R (1985) Isolation and sequence of a cDNA encoding the major structural protein of peripheral myelin. Cell 40:501-508.

López-Vales R, Navarro X, Shimizu T, Baskakis C, Kokotos G, Constantinou-Kokotou V, Stephens D, Dennis EA, David S (2008) Intracellular phospholipase A (2) group IVA and group VIA play important roles in Wallerian degeneration and axon regeneration after peripheral nerve injury. Brain 131:2620-2631

Ma ZQ, Dasari S, Chambers MC, Litton MD, Sobecki SM, Zimmerman LJ, Halvey PJ, Schilling B, Drake PM, Gibson BW, Tabb DJ (2009). IDPicker 2.0: Improved protein assembly with high discrimination peptide identification filtering. J Proteome Res 8:3872-3881.

Mackinnon SE (1989) New directions in peripheral nerve surgery. Ann Plast Surg 22:257-273.

Madison RD, Zomorodi A, Robinson GA (2000) Netrin-1 and peripheral nerve regeneration in the adult rat. Exp Neurol 161:563-570.

Martinez JA, Masaki K, Anand K (2015) Intrinsic facilitation of adult peripheral nerve regeneration by the Sonic hedgehog morphogen. Exp Neurol 271:493-505.

Matsunaga E, Sanae M, Michio T, Miki T, Atsushi I (2015) Periostin, a neurite outgrowth-promoting factor, is expressed at high levels in the primate cerebral cortex. Dev Growth Differ 57:200-208.

Monk KR, Oshima K, Jors S, Heller S, Talbot WS (2011) Gpr126 is essential for peripheral nerve development and myelination in mammals. Development 138:2673-2680.

Monnier PP, D'Onofrio PM, Magharious M, Hollander AC, Tassew N, Szydlowska K, Tymianski M, Koeberle PD (2011) Involvement of caspase-6 and caspase-8 in neuronal apoptosis and the regenerative failure of injured retinal ganglion cells. J Neurosci 31:10494-10505.

Nelder JA, Wedderburn RWM (1972) Generalized linear models. J R Statist Soc A 135:370-384

Newbern JM, Snider WD, Bers ERK (2012) Schwann cells coordinate nerve regeneration. Neuron 73:623-626.

Newman J, Verity A (1996) Ciliary neurotrophic factor enhances peripheral nerve regeneration. Arch Otolaryngol Head Neck Surg 122:399-403.

Nguyen LS, Jolly L, Shoubridge C, Shoubridge WK, Chan L, Huang F, Laumonnier MR (2012) Transcriptome profiling of UPF3B/NMD-deficient lymphoblastoid cells from patients with various forms of intellectual disability. Mol Psychiatr 17:1103-1115.

Pardo E, Barake F, Godoy JA, Oyanadel C, Espinoza S, Metz C, Retamal C, Massardo L, Tapia-Rojas C, Inestrosa NC, Soza A, González A (2019) GALECTIN-8 is a neuroprotective factor in the brain that can be neutralized by human autoantibodies. Mol Neurobiol 56:7774-7788.

Parrinello S, Napoli I, Ribeiro S, Wingfield F, Marina D, Parkinson DB, Doddrell RDS, Nakayama M, Adams RH, Lloyd AC (2010) EphB signaling directs peripheral nerve regeneration through Sox2-dependent Schwann cell sorting. Cell 43:145-155.

Raimondo TM, Li HH, Kwee BJ, Kinsley S, Budina E, Anderson EM, Doherty EJ, Talbot SG, Mooney DJ (2019) Combined delivery of VEGF and IGF-1 promotes functional innervation in mice and improves muscle transplantation in rabbits. Biomaterials 216:119246.

Ramaglia VM, Martijn RT, Maryla DK, Ruud W, Miriam AV, Rosalind HM, Bryan PM, Frank B (2009) Complement inhibition accelerates regeneration in a model of peripheral nerve injury. Mol Immunol 47:302-309.

Ren F, Zhang H, Qi C, Gao ML, Wang H, Li XQ (2015) Blockade of transient receptor potential cation channel subfamily V member 1 promotes regeneration after sciatic nerve injury. Neural Regen Res 10:1324-1331.

Roet KC, Franssen EH, deBree FM, Essing AH, Zijlstra SJJ, Fagoe ND, Eggink HM, Eggers R, Smit AB, van Kesteren RE, Verhaagen J (2013) A multilevel screening strategy defines a molecular fingerprint of proregenerative olfactory ensheathing cells and identifies SCARB2, a protein that improves regenerative sprouting of injured sensory spinal axons. J Neurosci 33:11116-11135.

Rotshenker S (2011) Wallerian degeneration: the innate-immune response to traumatic nerve injury. J Neuroinflammation 8:109.

Sahenk Z, Seharaseyon J, Mendell JR (1994) CNTF potentiates peripheral nerve regeneration. Brain Res 655:246-250.

Saito H, Kanje M, Dahlin LB (2009) Delayed nerve repair increases number of caspase 3 stained Schwann cells. Neurosci Lett 456:30-33.

Samii A, Carvalho GA, Samii M (2003) Brachial plexus injury: factors affecting functional outcome in spinal accessory nerve transfer for the restoration of elbow flexion. J Neurosurg 98:307-312.

Sbai O, Devi TS, Melone MA, Feron F, Khrestchatisky M, Singh LP, Perrone L (2010) RAGE-TXNIP axis is required for S100B-promoted Schwann cell migration, fibronectin expression and cytokine secretion. J Cell Sci 123:4332-4339.

Scherer SS, Xu YT, Nelles E, Fischbeck K, Willecke K, Bone LJ (1998) Connexin32-null mice develop a demyelinating peripheral neuropathy. Glia 24:8-20.

Sendtner M, Holtmann B, Kolbeckt R, Thoenen H, Barde YA (1992) Brain-derived neurotrophic factor prevents the death of motoneurons in newborn rats after nerve section. Nature 360:757-759.

Seon JJ, Yeon KH, Seop SB, Lee AR, Yoon JH, Hahm TS, Lee JE (2018) Increased expression of the Cbl family of E3 ubiquitin ligases decreases Interleukin-2 production in a rat model of peripheral neuropathy. BMC Anesthesiol 18:87.

Shih CH, Lacagnina M, LeuerBisciotti K, Pröschel C (2014) Astroglial-derived periostin promotes axonal regeneration after spinal cord injury. J Neurosci 34:2438-2443.

Shimamura M, Taniyama Y, Katsuragi N, Koibuchi N, Kyutoku M, Sato N, Allahtavakoli M, Wakayama K, Nakagami H, Morishita R (2012) Role of central nervous system periostin in cerebral ischemia. Stroke 43:1108-1114.

Shin YK, Jang YS, Park JY, Park SY, Lee HJ, Suh DJ, Park HT (2013) The neuregulin-Rac-MKK7 pathway regulates antagonistic c-jun/krox20 expression in Schwann cell dedifferentiation. Glia 61:892-904.

Simon CM, Stefanie R, Jennifer M, Gunnersen BH, Carsten D, Benjamin D, Massimiliano BG (2015) Dysregulated IGFBP5 expression causes axon degeneration and motoneuron loss in diabetic neuropathy. Acta Neuropathol 130:373-387.

Sonigra RJ, Brighton PC, Jacoby J, Hall S, Wigley CB (1999) Adult rat olfactory nerve ensheathing cells are effective promoters of adult central nervous system neurite outgrowth in coculture. Glia 25:256-269.

Sulaiman OA, Midha R, Munro CA, Matsuyama T, Al-Majed A, Gordon T (2002) Chronic Schwann cell denervation and the presence of a sensory nerve reduce motor axonal regeneration. Exp Neurol 17:342-354.

Sulaiman W, Gordon T (2013) Neurobiology of peripheral nerve injury, regeneration, and functional recovery: from bench top research to bedside application. Ochsner J 13:100-108.

Tabb DL, Fernando CG, Chambers MC (2007) MyriMatch: highly accurate tandem mass spectral peptide identification by multivariate hypergeometric analysis. J Proteome Res 6:654-661.

Trimarco A, Maria GF, Valentina A, Alessandra L, Paola B, Giorgia D, Damiana P (2014) Prostaglandin D2 synthase/GPR44: a signaling axis in PNS myelination. Nat Neurosci 17:1682-1692.

Vergara D, Romano A, Stanca E, Pesa VL, Aloisi L, Domenico SD, Franck J, Cicalini I, Giudetti A, Storelli E, Pieragostino D, Fournier I, Sannino A, Salzet M, Cerri F, Quattrini A, Maffia M (2018) Proteomic expression profile of injured rat peripheral nerves revealed biological networks and processes associated with nerve regeneration. J Cell Physiol 233:6207-6223.

Vlachos A, Korkotian E, Schonfeld E, Copanaki E, DellerT, Segal M (2009) Synaptopodin regulates plasticity of dendritic spines in hippocampal neurons. J Neurosci 9:1017-1033.

Wei S, Liang XZ, Hu Q, Wang WS, Xu WJ, Cheng XQ, Peng J, Guo QY, Liu SY, Jiang W, Ding X, Han GH, Liu P, Shi CH, Wang Y (2020) Different protein expression patterns in rat spinal nerves during Wallerian degeneration assessed using isobaric tags for relative and absolute quantitation proteomics profiling. Neural Regen Res 15:315-323.

Wood JD, Landers JA, Bingley M, McDermott CJ, Thomas-McArthur V, Gleadall LJ, Shaw PJ, Cunliffe VT (2006) The microtubule-severing protein Spastin is essential for axon outgrowth in the zebrafish embryo. Hum Mol Genet 15:2763-2771.

Wu P, Spinner RJ, Gu YD, Yaszemski MJ, Windebank AJ, Wang H (2013) Delayed repair of the peripheral nerve: a novel model in the rat sciatic nerve. J Neurosci Meth 214:37-44.

Yi S, Zhang HH, Gong LL, Wu JC, Zha GB, Zhou SL, Gu XS, Yu B (2015) Deep sequencing and bioinformatic analysis of lesioned sciatic nerves after crush injury. PLoS One 10:e0143491.

Zhang R, Zhang F, Li X, Huang S, Zi X, Liu T, Liu S, Li X, Xia K, Pan Q, Tang B (2014) A novel transgenic mouse model of Chinese Charcot-Marie-Tooth disease type 2L. Neural Regen Res 9:413-419.

Additional Table 1 Differentially expressed key proteins relevant to the inflammatory response process in the chronic denervation (delayed repair) and the non-chronic denervation (immediate repair) groups

Key proteins	IS-IC (FC)	DS-DC (FC)	IS-DS (FC)
CD63	20.09	1.33	14.89
IKBKG	16.45	2.83	4.51
CBL	-2.54	-4.64	1.95
MPZ	-1.39	-14.10	12.57
S100A8	-6.08	26.13	-30.77
S100A9	-8.09	18.16	-20.49
LIMK1	-1.37	-4.64	3.85
RAB27A	7.13	12.92	-0.91
SFRP1	6.19	13.60	-1.56
POSTN	12.52	12.77	-6.13
PTGDS	-11.20	-17.76	5.83
PLA2G4A	-12.50	20.76	-26.92

DC: delayed repair contralateral side; DS: delayed repair surgery side; FC: fold change; IC: immediate repair contralateral side; IS: immediate repair surgery side.

Additional Table 2 Differentially expressed key proteins relevant to the cell proliferation process in the chronic denervation (delayed repair) and the non-chronic denervation (immediate repair) groups

Key proteins	IS-IC (FC)	DS-DC (FC)	IS-DS (FC)
SPAST	-15.54	-10.36	6.82
ARHGAP24	17.23	1.28	12.30
EGR2	17.33	12.93	1.05
CD63	20.09	1.33	14.89
MADD	-3.03	-21.44	18.60
IGF1R	-8.59	-19.89	10.69
MPZ	-1.39	-14.09	12.57
DHH	-2.41	-4.87	2.14
HSPB8	-2.57	-4.70	1.87
CBL	-2.54	-4.64	1.95
GJB1	-1.85	-4.51	2.66
CASP6	-5.32	12.26	-8.86
CASP3	10.25	14.70	0.62
S100A8	-6.08	26.13	-30.77
S100A9	-8.09	18.16	-20.49
IGFBP5	0.12	20.10	-18.54
LIMK1	-1.37	-4.64	3.85
RAB27A	7.13	12.92	-0.91
SFRP1	6.19	13.60	-1.56
POSTN	12.52	12.77	-6.13
SHH	-4.81	-10.58	5.10
MAPK11	-14.80	-35.17	19.48
PTGDS	-11.20	-17.76	5.83
APOD	4.76	4.80	-0.44
MSLN	-11.33	13.88	-23.77

DC: delayed repair contralateral side; DS: delayed repair surgery side; FC: fold change; IC: immediate repair contralateral side; IS: immediate repair surgery side.

Additional Table 3 Differentially expressed key proteins relevant to the cell apoptosis process in the chronic denervation (delayed repair) and the non-chronic denervation (immediate repair) groups

Key proteins	IS-IC (FC)	DS-DC (FC)	IS-DS (FC)
SMURF1	-17.98	-7.75	-9.18
NFIB	-11.33	14.58	-24.48
IKBKG	16.45	2.83	4.51
EGR2	17.33	12.93	1.05
MADD	-3.03	-21.44	18.60
IGF1R	-8.59	-19.89	10.69
MPZ	-1.39	-14.10	12.57
LGALS8	0.77	-13.86	8.48
PAK3	-3.04	-5.26	2.19
HSPB8	-2.57	-4.70	1.87
CNTF	-0.10	-4.18	2.20
CBL	-2.54	-4.64	1.95
GJB1	-1.85	-4.51	2.66
CASP6	-5.32	12.26	-8.86
CASP3	10.25	14.70	0.62
RAB27A	7.13	12.92	-0.91
SFRP1	6.19	13.60	-1.56
S100A9	-8.09	18.16	-20.49
IGFBP5	0.12	20.10	-18.54
C6	13.77	21.37	-0.74
S100A8	-6.08	26.13	-30.77
POSTN	12.52	12.77	-6.13
CAMKK1	-4.28	-18.65	14.79
MAPK11	-14.80	-35.17	19.48
PTGDS	-11.20	-17.76	5.83
SHH	-4.81	-10.58	5.10
APOD	4.76	4.80	-0.44

DC: delayed repair contralateral side; DS: delayed repair surgery side; FC: fold change; IC: immediate repair contralateral side; IS: immediate repair surgery side.

Additional Table 4 Differentially expressed key proteins relevant to the cell migration process of the chronic denervation (delayed repair) and the non-chronic denervation (immediate repair) groups

Key proteins	IS-IC (FC)	DS-DC (FC)	IS-DS (FC)
CD63	20.09	1.33	14.89
IKBKG	16.45	2.83	4.51
EGR2	17.33	12.93	1.05
MPZ	-1.39	-14.10	12.57
LIMK1	-1.37	-4.64	3.85
RAB27A	7.13	12.92	-0.91
SFRP1	6.19	13.60	-1.56
S100A8	-6.08	26.13	-30.77
S100A9	-8.09	18.16	-20.49
C6	13.77	21.37	-0.734
PTGDS	-11.20	-17.76	5.83
EPHB2	14.91	24.44	-2.94
ITGB2	22.91	17.93	0.40
TXNIP	20.81	17.54	-1.18
LYN	21.26	19.28	-1.59
ADGRG6	-10.54	-17.48	7.17

DC: delayed repair contralateral side; DS: delayed repair surgery side; FC: fold change; IC: immediate repair contralateral side; IS: immediate repair surgery side.

Additional Table 5 Differentially expressed key proteins relevant to the axon regeneration process of the chronic denervation (delayed repair) and the non-chronic denervation (immediate repair) groups

Key proteins	IS-IC (FC)	DS-DC (FC)	IS-DS (FC)
EGR2	17.33	12.93	1.05
SPAST	-15.54	-10.36	6.83
IGF1R	-8.59	-19.89	10.69
MPZ	-1.39	-14.10	12.57
SHH	-4.81	-10.58	5.10
PAK3	-3.04	-5.26	2.19
HSPB8	-2.57	-4.70	1.87
LIMK1	-1.37	-4.64	3.85
GJB1	-1.85	-4.50	2.66
CNTF	-0.10	-4.18	2.20
CASP6	-5.31	12.26	-8.86
CASP3	10.25	14.70	0.62
CAMKK1	-4.28	-18.65	14.79
SYNPO	15.54	17.40	-6.99
NTN1	16.96	13.87	-1.20
SMURF1	-17.98	-7.75	-9.18
ARPP19	-12.67	-26.14	8.56

DC: delayed repair contralateral side; DS: delayed repair surgery side; FC: fold change; IC: immediate repair contralateral side; IS: immediate repair surgery side.

Additional Table 6 Differentially expressed key proteins relevant to the lipid metabolism process of the chronic denervation (delayed repair) and the non-chronic denervation (immediate repair) groups
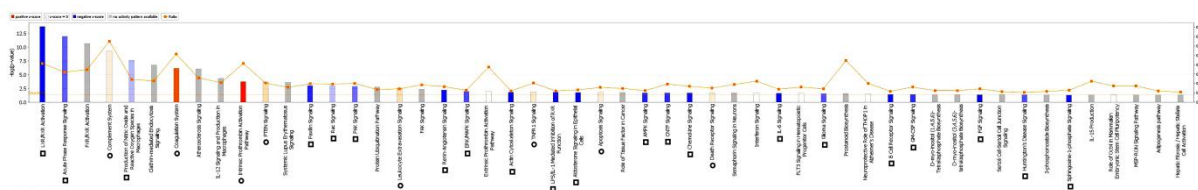
Key proteins	IS-IC (FC)	DS-DC(FC)	IS-DS (FC)
IGF1R	-8.59	-19.89	10.69
PTGDS	-11.20	-17.76	5.83
TRPV1	-8.14	-14.97	7.09
LGALS8	0.77	-13.86	8.48
DHH	-2.41	-4.87	2.14
LIMK1	-1.37	-4.64	3.85
CBL	-2.54	-4.64	1.95
CNTF	-0.10	-4.18	2.20
RAB27A	7.13	12.92	-0.91
CASP3	10.25	14.70	0.62
S100A9	-8.09	18.16	-20.49
S100A8	-6.08	26.13	-30.77
APOD	4.76	4.80	-0.44

DC: delayed repair contralateral side; DS: delayed repair surgery side; FC: fold change; IC: immediate repair contralateral side; IS: immediate repair surgery side.
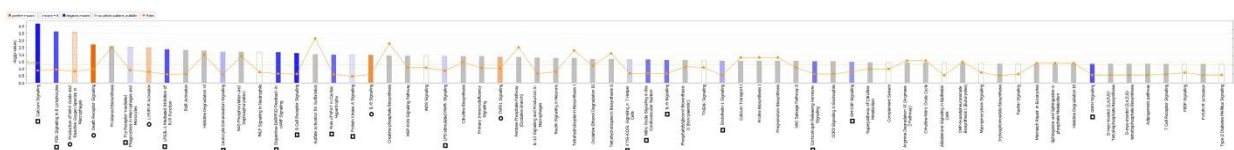
Additional Figure 1 Significantly regulated pathways in the immediate repair group.

Sixty-five canonical pathways were identified by IPA pathway analysis. Five pathways (denoted by a circle that precedes the pathway name) were predicted to be activated, and 17 pathways (denoted by a square that precedes the pathway name) were predicted to be inhibited. –log (P value) was calculated by Fisher's exact test right-tailed. Orange colored bars indicate predicted pathway activation with a positive z-score (the circle preceding the pathway way name indicates that particular pathway is activated). Blue colored bars indicate predicted pathway inhibition with a negative z-score (the square preceding the pathway way name indicates that particular pathway is inhibited). The orange points connected by a thin line represent the Ratio. The ratio was calculated as follows: the number of proteins in a given pathway that met the cutoff criteria, divided by the total number of proteins that make up that pathway and that are in the reference protein set.

Additional Figure 2 Significantly regulated pathways in the delayed repair group.

Fifty-two canonical pathways were identified by IPA pathway analysis. Eight signaling pathways (denoted by a circle that precedes the pathway name) were predicted to be activated, and 21 signaling pathways (denoted by a square that precedes the pathway name) were predicted to be inhibited. –log (P value) was calculated by Fisher's exact test right-tailed. Orange colored bars indicate predicted pathway activation with a positive z-score (the circle preceding the pathway way name indicates that particular pathway is activated). Blue colored bars indicate predicted pathway inhibition with a negative z-score (the square preceding the pathway way name indicates that particular pathway is inhibited). The orange points connected by a thin line represent the Ratio. The ratio was calculated as follows: the number of proteins in a given pathway that met the cutoff criteria, divided by the total number of proteins that make up that pathway and that are in the reference protein set.